Journal of Organometallic Chemistry, 394 (1990) 87–97
Elsevier Sequoia S.A., Lausanne
JOM 21125

Synthesis and reactivity of bis(trimethylsilyl)cyclopentadienyl samarium complexes including the X-ray crystal structure of $[(Me_3Si)_2C_5H_3]_3Sm$ *,**

William J. Evans *, **Roy A. Keyer and Joseph W. Ziller**
Department of Chemistry, University of California — Irvine, Irvine, CA 92717 (U.S.A.)

(Received February 13th, 1990)

Abstract

$SmI_2(THF)_2$ reacts with two equivalents of $K[1,3\text{-}(Me_3Si)_2C_5H_3]$ to form $[(Me_3Si)_2C_5H_3]_2Sm(THF)$ (**1**). **1** can be desolvated by sublimation at 80 °C and 4×10^{-6} Torr to give $[(Me_3Si)_2C_5H_3]_2Sm$ (**2**). **1** polymerizes ethylene and reacts under 90 psi of CO to form $[(Me_3Si)_2C_5H_3]_3Sm$ (**3**) which can also be synthesized directly from $SmCl_3$ and $KC_5H_3(SiMe_3)_2$. **3** crystallizes from toluene in space group $P2_1/c$ with unit cell dimensions $a = 17.961(3)$, $b = 13.748(2)$, $c = 19.327(3)$ Å, $\beta = 112.80(1)°$, $V = 4397.9(11)$ Å^3 and $Z = 4$ for $D_{calcd} = 1.17$ g cm^{-3}. Least squares refinement on the basis of 6173 observed reflections led to a final R_F value of 5.3%. The three $1,3\text{-}(Me_3Si)_2C_5H_3$ ring-centroids form a trigonal plane around the samarium center with an average Sm–C(ring) distance of 2.76(4) Å. The silyl-substituted part of each ring is tilted away from the samarium atoms such that individual Sm–C distances vary from 2.698(5) to 2.806(5) Å within the same ring.

Introduction

The discovery of the soluble, organometallic Sm^{II} reagents $(C_5Me_5)_2Sm(THF)_2$ [1,2] and $(C_5Me_5)_2Sm$ [3,4] has provided access to a variety of unusual, lanthanide-based, multiple bond transformation reactions [5–9]. For example, carbon monoxide can be reductively homologated to the ketenecarboxylate, $O_2CC{=}C{=}O^{2-}$, by $(C_5Me_5)_2Sm(THF)_2$ (eq. 1) [6]. Investigation of the reduction of CO by other

---

* Dedicated to Professor F.G.A. Stone, an inspiration to all synthetic inorganic chemists, on the occasion of his 65th birthday.

** Reported in part at the 196th Meeting of the American Chemical Society, Los Angeles, California, September 1988, INOR 250.

0022-328X/90/$03.50

soluble Sm^{II} reagents such as $SmI_2(THF)_2$ [10] and $[(Me_3Si)_2N]_2Sm(THF)_2$ [11] has not given analogous results [11,12]. In efforts to probe the importance of the C_5Me_5 ligand in these reactions, we have explored the utility of an alternative cyclopentadienyl ligand, the bulky, disubstituted ligand, 1,3-$(Me_3Si)_2C_5H_3$ [13–22], in organosamarium(II) chemistry. We report here on the synthesis of Sm^{II} complexes of this ligand, reactivity with ethylene and CO, and the formation and crystal structure of the tris(cyclopentadienyl) derivative, $[(Me_3Si)_2C_5H_3]_3Sm$.

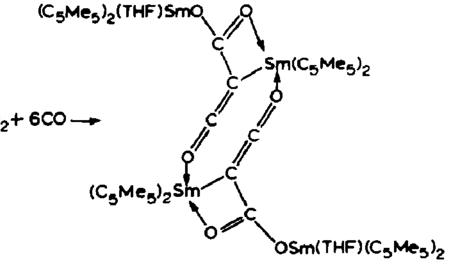

(1)

Experimental

The air- and moisture-sensitive compounds described below were handled under nitrogen using Schlenk, high-vacuum, and glovebox (Vacuum/Atmospheres HE-533 Dri-Lab) techniques. Physical measurements were obtained as previously described [23]. Tetrahydrofuran (THF), toluene, and hexane were distilled from sodium benzophenone ketyl. Benzene-d_6 and THF-d_8 were vacuum transferred from sodium benzophenone ketyl. Chlorotrimethylsilane was vacuum transferred from 4 Å molecular sieves. Potassium hydride (Aldrich) was washed with hexane and dried under vacuum. Ethylene (Matheson, polymer grade) was passed over manganese(II) oxide on vermiculite [24] and 4 Å molecular sieves prior to use. Carbon monoxide (Liquid Carbonic, research grade) was used as received. KC_5H_5 was made from KH and freshly cracked C_5H_6. $SmI_2(THF)_2$ [10], $SmCl_3$ [25] and $(C_5Me_5)_2Sm(THF)$ [26] were prepared as previously described. $KC_5H_3(SiMe_3)_2$ was prepared using a modification of the literature procedure [13,14] as described below.

$KC_5H_4SiMe_3$. In the glovebox, KC_5H_5 (5.33 g, 51.2 mmol), 200 mL of toluene, and a stir bar were placed in a 3-neck round bottom flask fitted with a nitrogen inlet, a stopper, and an addition funnel. Me_3SiCl (6.0 mL, 47.3 mmol) in 20 mL of toluene was placed in the addition funnel. The reaction vessel was removed from the glovebox, attached to a Schlenk line, and cooled to 0 °C. The Me_3SiCl solution was added dropwise over a period of 10 min, and the resulting solution was stirred. After 8 h, the reaction mixture was filtered to give a yellow solution of $C_5H_5SiMe_3$ in toluene which was identified by ^1H NMR (THF-d_8) [14].

The yellow toluene solution was placed in a Schlenk addition funnel and attached to a 500 mL Schlenk flask which contained KH (2.00 g, 49.9 mmol) and 150 mL of THF. The solution was added dropwise to the stirring suspension of KH over a period of one hour and the reaction was stirred overnight. Excess KH was removed by filtration and washed with THF to recover any product. Solvent was removed by rotary evaporation to give $KC_5H_4SiMe_3$ (7.20 g, 43.1 mmol, 90% yield).

$KC_5H_3(SiMe_3)_2$. In a manner similar to that given above, Me_3SiCl (6.0 mL, 47.3 mmol) was added to a THF solution of $KC_5H_4SiMe_3$ (7.20 g, 43.1 mmol).

After stirring for 8 h, the reaction mixture was filtered to remove KCl from the solution of $C_5H_4(SiMe_3)_2$, which was identified by ^1H NMR [14]. A THF solution of this compound was then reacted with KH (2.00 g, 49.9 mmol) as described above to yield $KC_5H_3(SiMe_3)_2$ (9.60 g, 38.5 mmol, 89% yield).

$[(Me_3Si)_2C_5H_3]_2Sm(THF)$ (1). In the glovebox, $SmI_2(THF)_2$ (1.5 g, 2.7 mmol) was added to a stirring solution of $KC_5H_3(SiMe_3)_2$ (1.4 g, 5.7 mmol) in 15 mL of THF. The purple reaction mixture was stirred for 8 h and then filtered. Solvent was removed in vacuo to leave a dark green oil, which was dissolved in 10 mL of hexane. The hexane was removed in vacuo to give dark green hexane insoluble solids which were washed with two 10 mL portions of hexane to give **1** (1.5 g, 2.3 mmol, 85%). Anal. Found: C, 48.46; H, 7.72; Si, 17.25; Sm, 23.35. $C_{26}H_{50}OSi_4Sm$ calcd.: C, 48.69; H, 7.86; Si, 17.51; Sm, 23.45%. ^1H NMR (THF-d_8): δ 19.87 (2H, C_5H_3), 5.34 (1H, C_5H_3), 2.42 (18H, CH_3). ^1H NMR (C_6D_6): δ 11.17 (18H, CH_3), 10.44 (2H, C_5H_3), −4.11 (2H, C_4H_8O), −5.12 (2H, C_4H_8O), −11.42 (1H, C_5H_3). ^{13}C NMR (THF-d_8): δ 17.48 (s, CH_3), −7.48 (d, $J = 152$ Hz, C_5H_3), −35.16 (d, $J = 148$ Hz, C_5H_3), −88.09 (s, C_5H_3). Magnetic susceptibility: $\chi_M = 4700 \times 10^{-6}$ cgs; $\mu_{eff} = 3.35$ μ_B. IR (KBr): 3030 m, 3020 m, 2950 s, 2900 s, 1750 w, br, 1580 w, br, 1030 m cm^{-1}.

$[(Me_3Si)_2C_5H_3]_2Sm$ (2). In the glovebox, **1** (193 mg, 0.30 mmol) was placed in a pyrex tube fitted with a high vacuum stopcock and the apparatus was then attached to a high vacuum line. The sublimation tube was evacuated to 4×10^{-6} Torr and heated to 80 °C. After 12 h, a dark green material had sublimed, which, by NMR spectroscopy, still contained coordinated THF. This material was re-sublimed under the same conditions to give THF-free **2** in 20–30% yield. ^1H NMR (C_6D_6): δ 12.90 (2H, C_5H_3), 10.36 (18H, CH_3), −17.45 (1H, C_5H_3).

$[(Me_3Si)_2C_5H_3]_3Sm$ (3). In the glovebox, $SmCl_3$ (100 mg, 0.390 mmol), $KC_5H_3(SiMe_3)_2$ (300 mg, 1.20 mmol), and 150 mL of toluene were placed in a Schlenk flask fitted with a reflux condensor. The reaction vessel was then attached to a Schlenk line and the reaction was heated at reflux for 16 h. The orange solution was brought back into the box and centrifuged to remove KCl. Solvent was removed in vacuo to yield **3** (292 mg, 0.373 mmol, 96%). ^1H NMR (C_6D_6): δ 23.20 (1H, C_5H_3), 18.63 (2H, C_5H_3), −1.85 (18H, CH_3). ^{13}C NMR (C_6D_6): δ 133.93 (d, $J = 163$ Hz, C_5H_3), 121.11 (d, $J = 162$ Hz, C_5H_3), 109.02 (s, C_5H_3), −3.62 (q, $J = 119$ Hz, CH_3). IR (KBr): 2950 m, 2900 m, 1550 w, 1440 m, 1400 m, 1320 m, 1250 s, 1210 m, 1070 s, 1030 s, 920 m, 800 br, 690 w, 620 w cm^{-1}. Magnetic susceptibility: $\chi_M = 1448 \times 10^{-6}$ cgs; $\mu_{eff} = 1.86$ μ_B.

Reaction of 1 with ethylene. A green solution of **1** (55 mg, 86 mmol) in 10 mL of toluene was placed in a Schlenk flask and attached to Schlenk line charged with ethylene. The reaction vessel was evacuated and then backfilled with ethylene. Gas uptake began immediately and solids soon formed in the flask. After 2.5 h, the solution was still green. The flask was evacuated and the resulting solids were dried in vacuo to give 6.3 g of off-white polymer containing pale green samarium residues (~ 1000 turnovers/h). Ethylene was polymerized by $(C_5Me_5)_2Sm(THF)$ (41 mg, 83 mmol) under the same conditions to form 0.42 g of polymer in 1.0 h (~ 170 turnovers/h). The samarium complex became yellow during the polymerization.

Reaction of 1 with CO. In the glovebox, **1** (212 mg, 0.339 mmol) was placed in a 3 oz. Lab-Crest (Fischer–Porter) glass pressure reaction vessel containing a stir bar and 20 mL of hexane. The apparatus was then attached to a high-pressure manifold as previously described [27] and pressurized to 90 psi with CO. The green hexane suspension was allowed to stir for 12 h and then vented to 1 atm. The reaction mixture was brought into the glovebox, centrifuged, and stripped of solvent to give 187 mg of a red-brown material. ^1H NMR spectroscopy showed that a single primary $C_5H_3(SiMe_3)_2$ complex was present. Crystals of this product were grown from toluene at −35 °C and identified by X-ray crystallography as $[(Me_3Si)_3C_5H_3]_3Sm$. A control reaction involving nitrogen instead of CO was run analogously. No color change occurred and 1 was recovered quantitatively after 12 h.

X-ray diffraction study of $[(Me_3Si)_2C_5H_3]_3Sm$. A reddish-yellow crystal of approximate dimensions 0.33 × 0.43 × 0.50 mm was mounted in a thin-walled glass capillary under an inert (N_2) atmosphere and aligned on a Nicolet P3 automated four-circle diffractometer. Laue symmetry determination, crystal class, unit cell parameters and the crystal's orientation matrix were carried out by previously described techniques similar to those of Churchill [28]. Room temperature (22 °C) intensity data were collected using the θ–2θ scan technique with Mo-K_α radiation under the conditions given in Table 1. All 7787 data were corrected for the effects of absorption and for Lorentz and polarization effects and placed on an approximately absolute scale by means of a Wilson plot. A preliminary data set revealed the systematic extinctions $0k0$ for $k = 2n + 1$ and $h0l$ for $l = 2n + 1$; the diffraction

Table 1

Crystal data on $[(Me_3Si)_2C_5H_3]_3Sm$ (3)

Formula: $C_{33}H_{63}Si_6Sm$
Fw: 778.9
Temperature (K): 295
Crystal system: Monoclinic
Space group: $P2_1/c$ [C^5_{2h}; No. 14]
$a = 17.961(3)$ Å
$b = 13.748(2)$ Å
$c = 19.327(3)$ Å
$\beta = 112.80(1)°$
$V = 4397.9(11)$ Å^3
$Z = 4$
D_{calcd}, g/cm^3 = 1.17
Diffractometer: Nicolet P3 (R3m/V System)
Radiation: Mo-K_α (λ = 0.710730 Å)
Monochromator: Highly oriented graphite
Data collected: $+h$, $+k$, $\pm l$
Scan type: Coupled θ(crystal) − 2θ(counter)
Scan width: Symmetrical $[2\theta(K\alpha_1) - 1.2] \rightarrow [2\theta(K\alpha_2) + 1.2]$
Scan speed: 4.0 deg min^{-1} (in 2θ)
2θ Range: 4.0 to 50.0°
μ(Mo-K_α), cm^{-1} = 15.2
Absorption correction: Semi-empirical (ψ-scan method)
Total reflections: 7787
Reflections with $|F_o| > 2.0\sigma(|F_o|)$: 6173
No. of variables: 361
$R_F = 5.3\%$; $R_{wF} = 4.9\%$
Goodness of fit: 1.18

symmetry was $2/m$. The centrosymmetric monoclinic space group $P2_1/c$ [C^5_{2h}; No. 14] is thus uniquely defined.

All crystallographic calculations were carried out using either our locally modified version of the UCLA Crystallographic Computing Package [29] or the SHELXTL PLUS program set [30]. The analytical scattering factors for neutral atoms were used throughout the analysis [31a]; both the real (Δf) and imaginary ($i\,\Delta f''$) components of anomalous dispersion [31b] were included. The weighting scheme using $p = 0.05$ has been previously described [32].

Table 2

Final fractional coordinates for $[(Me_3Si)_2C_5H_3]_3Sm$ (3)

Atom	*x*	*y*	*z*
Sm(1)	0.24957(2)	0.08587(2)	0.30047(1)
Si(1)	0.3204(1)	−0.2058(1)	0.3776(1)
Si(2)	0.1889(1)	0.0954(2)	0.4965(1)
Si(3)	0.3334(2)	0.3747(2)	0.3731(1)
Si(4)	0.4771(1)	0.0721(2)	0.2698(1)
Si(5)	0.0248(1)	0.2416(2)	0.2036(1)
Si(6)	0.1639(1)	−0.0614(1)	0.0902(1)
C(1)	0.2599(4)	−0.0939(4)	0.3698(3)
C(2)	0.2743(4)	−0.0261(4)	0.4289(3)
C(3)	0.2058(4)	0.0298(4)	0.4188(3)
C(4)	0.1451(3)	−0.0034(4)	0.3505(3)
C(5)	0.1784(4)	−0.0778(4)	0.3219(3)
C(6)	0.2850(6)	−0.2972(6)	0.4288(6)
C(7)	0.4292(5)	−0.1851(6)	0.4318(5)
C(8)	0.3036(6)	−0.2581(6)	0.2843(5)
C(9)	0.2859(5)	0.1433(6)	0.5657(4)
C(10)	0.1522(7)	0.0042(8)	0.5457(5)
C(11)	0.1144(6)	0.1946(8)	0.4630(5)
C(12)	0.3501(4)	0.2450(4)	0.3563(3)
C(13)	0.3712(4)	0.2116(4)	0.2969(3)
C(14)	0.4079(4)	0.1187(5)	0.3128(3)
C(15)	0.4106(3)	0.0947(5)	0.3861(3)
C(16)	0.3765(4)	0.1706(5)	0.4118(3)
C(17)	0.2814(7)	0.4407(5)	0.2851(5)
C(18)	0.4353(7)	0.4283(7)	0.4182(6)
C(19)	0.2786(7)	0.3893(7)	0.4360(6)
C(20)	0.4476(5)	0.1211(7)	0.1738(5)
C(21)	0.4838(6)	−0.0624(6)	0.2695(5)
C(22)	0.5792(5)	0.1185(7)	0.3302(6)
C(23)	0.1093(4)	0.1690(5)	0.1971(3)
C(24)	0.1040(3)	0.0700(4)	0.1754(3)
C(25)	0.1650(4)	0.0450(4)	0.1496(3)
C(26)	0.2083(4)	0.1326(5)	0.1530(3)
C(27)	0.1760(4)	0.2071(4)	0.1822(3)
C(28)	0.0582(5)	0.3455(7)	0.2691(5)
C(29)	−0.0422(5)	0.1634(6)	0.2318(5)
C(30)	−0.0328(5)	0.2890(6)	0.1077(4)
C(31)	0.2690(5)	−0.0987(6)	0.1071(5)
C(32)	0.1053(6)	−0.1630(6)	0.1068(4)
C(33)	0.1142(5)	−0.0217(6)	−0.0100(4)

The structure was solved by direct methods (SHELXTL PLUS); the position of the samarium atom was located from an E-map. Subsequent difference-Fourier syntheses revealed the positions of all remaining nonhydrogen atoms. Full-matrix least-squares refinement of positional and thermal parameters led to convergence with $R_F = 5.3\%$, $R_{wF} = 4.9\%$ and GOF = 1.18 for 361 variables refined against those 6173 data with $F^2 > 1.0\ \sigma(F^2)$. ($R_F = 3.5\%$, $R_{wF} = 4.2\%$ for those 4904 data with $F^2 > 3.0\ \sigma(F^2)$). Hydrogen atoms were located from difference-Fourier syntheses to determine their geometry. Their positions and thermal parameters were then fixed using the SHELXTL PLUS program XP (d(C–H) = 0.95 Å) [33]. A final difference-Fourier synthesis showed no significant features. Final fractional coordinates are given in Table 2.

Results

Synthesis

$[KC_5H_3(SiMe_3)_2]$ reacts with $SmI_2(THF)_2$ in THF to form $[(Me_3Si)_2C_5H_3]_2Sm(THF)$ (**1**) (eq. 2) in a reaction analogous to the synthesis of $(C_5Me_5)_2Sm(THF)_2$ [2].

$$SmI_2(THF)_2 + 2\ KC_5H_3(SiMe_3)_2 \rightarrow \left[(Me_3Si)_2C_5H_3\right]_2Sm(THF) + 2\ KI \qquad (2)$$

1 was characterized by elemental analysis, NMR and IR spectroscopy, and magnetic moment measurement. Complete elemental analysis and integration of the broad THF resonances at δ −4.11 and −5.12 ppm in the ^{1}H NMR spectrum of **1** in C_6D_6 suggested that this complex was the monosolvate shown in eq. 2 rather than the disolvate analogous to $(C_5Me_5)_2Sm(THF)_2$. The green color of **1** in the solid-state was also consistent with a monosolvated form since the analogous C_5Me_5 monosolvate, $(C_5Me_5)_2Sm(THF)$, is also green [26]. In contrast, the C_5Me_5 disolvate $(C_5Me_5)_2Sm(THF)_2$ is purple, a color which matches the color of **1** in THF. The color criterion is not definitive, however, since unsolvated $(C_5Me_5)_2Sm$ is green [3,4] and the tetrahydropyran monosolvate, $(C_5Me_5)_2Sm(OC_5H_{10})$, is brown [26].

Complex **1** can be desolvated to form the green complex $[(Me_3Si)_2C_5H_3]_2Sm$ (**2**) by the repeated sublimation of **1** at ~ 80 °C. In comparison, the conversion of $(C_5Me_5)_2Sm(THF)_2$ to $(C_5Me_5)_2Sm$ requires 4 h at 80 °C, followed by 8 h at 100 °C [3,4]. The bis(trimethylsilyl)cyclopentadienyl ligand apparently increases the volatility of **2** compared to $(C_5Me_5)_2Sm$. Since **1** is also more volatile than $(C_5Me_5)_2Sm(THF)$ [26], the solvated **1** can sublime without losing solvent. Hence, multiple sublimations are needed in order to obtain a sublimate containing a sample of **2** which is free of **1**. The solubility of **1** in hexane, 9 mg/mL, is comparable to that of $(C_5Me_5)_2Sm(THF)$, 8 mg/mL.

Reactivity

1 polymerizes ethylene in a reaction analogous to that observed previously for $(C_5Me_5)_2Sm(THF)_2$ [1,34] and $(C_5Me_5)_2Sm$ [12,35]. Gas uptake begins immediately and solid polymer begins to appear shortly after the reaction is initiated. The turnover rate of approximately 1000 turnovers/h was not optimized. The reaction of $(C_5Me_5)_2Sm(THF)$ with ethylene was conducted to allow a direct comparison and a slower rate, ~ 170 turnovers/h, was found.

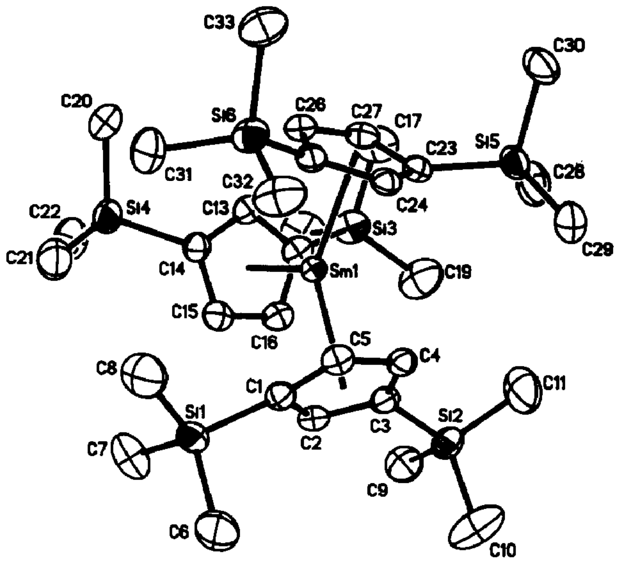

Fig. 1. ORTEP diagram of $[(Me_3Si)_2C_5H_3]_3Sm$ (3) with thermal ellipsoids at the 30% probability level.

The reaction of **1** with CO was examined to see how it compared with reaction 1 above. When a green suspension of **1** in hexane is placed under 90 psi of CO, an orange hexane soluble compound forms over a 12 h period. The color change was indicative of an oxidation from Sm^{II} to Sm^{III} [36]. The ^1H NMR spectrum of the solid product, **3**, showed that the bis(trimethylsilyl)cyclopentadienyl ligand was still coordinated to samarium, but no CO stretches were observed in the IR spectrum. Since the spectroscopic and analytical data were not structurally definitive, single crystals of **3** were grown and examined by X-ray crystallography. In this way, **3** was identified as the tris(cyclopentadienyl) complex, $[(Me_3Si)_2C_5H_3]_3Sm$. **3** can also be synthesized directly from $SmCl_3$ and $KC_5H_3(SiMe_3)_2$ in toluene at reflux as shown in reaction 3.

$$SmCl_3 + 3\ KC_5H_3(SiMe_3)_2 \xrightarrow{24\text{ h}} [(Me_3Si)_2C_5H_3]_3Sm + 3\ KCl \tag{3}$$

X-ray crystal structure

The structure of **3** is shown in Fig. 1 and selected bond distance and angle data are given in Table 3. Crystals of **3** are isomorphous with those of $[(Me_3Si)_2C_5H_3]_3Th$ (**4**) [19] and the overall structures are similar. In each molecule, three ring centroids

Table 3

Selected bond distances (Å) and angles (deg) in $[(Me_3Si)_2C_5H_3]_3Sm$ (3)

Sm(1)–C(1)	2.783(6)	Sm(1)–C(2)	2.806(5)
Sm(1)–C(3)	2.800(5)	Sm(1)–C(4)	2.714(5)
Sm(1)–C(5)	2.698(5)	Sm(1)–C(12)	2.775(6)
Sm(1)–C(13)	2.807(5)	Sm(1)–C(14)	2.797(6)
Sm(1)–C(15)	2.722(6)	Sm(1)–C(16)	2.717(6)
Sm(1)–C(23)	2.783(6)	Sm(1)–C(24)	2.799(5)
Sm(1)–C(25)	2.774(5)	Sm(1)–C(26)	2.729(5)
		Sm(1)–C(27)	2.722(6)
Cent(1)–Sm(1)–Cent(2)	119.9	Cent(1)–Sm(1)–Cent(3)	120.0
Cent(2)–Sm(1)–Cent(3)	120.1	C(1)–Si(1)–C(6)	107.0(3)

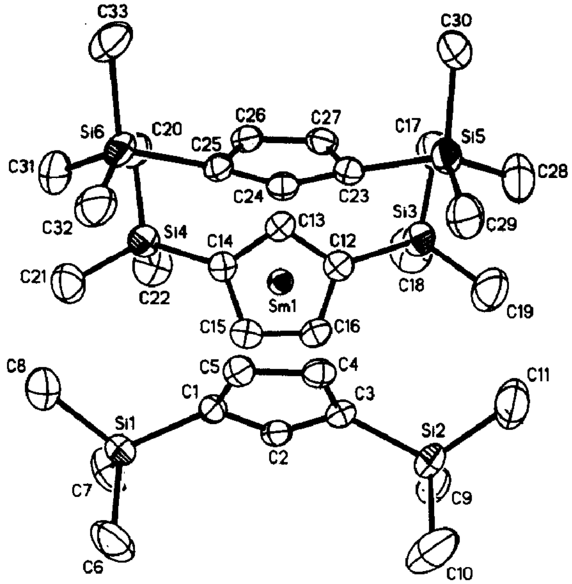

Fig. 2. Alternative view of $[(Me_3Si)_2C_5H_3]_3Sm$ showing the orientation of the Me_3Si groups.

define a trigonal plane with (ring centroid)–metal–(ring centroid) angles which average 120°. In 3, the range of these angles is very narrow: 120.1, 120.0 and 119.9°. Figure 2 shows the relative orientation of the bulky Me_3Si groups in 3. A view of complex 4 from this perspective shows a similar arrangement. The three Me_3Si groups on each side of Fig. 2 are oriented to be as far apart as possible and form a triangular array. The six silicon atoms define a trigonal prism. The dihedral angle between the two triangles of silicon atoms is 0.7° compared to 0° for a perfect trigonal prism.

The average Sm–C distance in 3 is 2.76(4) Å compared to a 2.80(2) Å average in 4. Direct comparisons of these M–C distances using Shannon's radii [37] are not possible since no values for Th^{3+} are given. However, the following data suggest that Th^{3+} should be larger than Sm^{3+}. Since six-coordinate U^{3+} is 0.135 Å larger than six-coordinate U^{4+} according to Shannon [37], the radius of nine-coordinate Th^{3+} is expected to be larger than the 1.09 Å radius of nine-coordinate Th^{4+}. A 0.135 increment on the 1.09 Å Th^{4+} radius gives an extrapolated Th^{3+} nine-coordinate radius of 1.225 Å compared to the 1.132 Å radius of nine-coordinate Sm^{3+}.

The Sm–C average distance for 3 is derived from a wide range of distances with extremes of 2.698(5) and 2.807(5) Å. The longest Sm–C distance in each ring involves the carbon atom between the two Me_3Si-substituted carbons, i.e., the sterically most crowded positions C(2), C(13) and C(24). The next longest Sm–C distances in each ring involve the Me_3Si-substituted carbon atoms C(1), C(3), C(12), C(14), C(23) and C(25). The shortest distances involve the remaining carbons which are least sterically congested. Hence, each ring tilts away from the metal to allow the Me_3Si groups to be further apart. This pattern of long and short M–C distances is not found in 4, however. The range of Th–C distances in 4, 2.77(3)–2.85(2) Å, is smaller and no regular pattern of long distances associated with the sterically crowded positions is observable in 4.

Discussion

The $(Me_3Si)_2C_5H_3$ ligand was originally introduced into *f*-element chemistry to provide "distinct and complementary features to C_5Me_5" [15], a bulky cyclopentadienyl ligand which has proven extremely useful in this field [36,38–40]. The $(Me_3Si)_2C_5H_3$ ligand, like C_5Me_5, has provided steric bulk and solubility to systems which could not be easily developed with simple C_5H_5 ligands. For example, both ligands have been useful in developing early lanthanide chemistry [15–17,41–47].

For Sm^{II}, the bis(trimethylsilyl)cyclopentadienyl ligand provides soluble divalent complexes analogous to C_5Me_5 species and in contrast to the insoluble C_5H_5 complex, $[(C_5H_5)_2Sm(THF)]_n$ [48]. The reactivity of $[(Me_3Si)_2C_5H_3]_2Sm(THF)$ with ethylene is similar to that of $(C_5Me_5)_2Sm(THF)$ in that both Sm^{II} complexes form polymers. The higher rate observed for **1** compared to $(C_5Me_5)_2Sm(THF)$ may arise because the bulkiness of the $(Me_3Si)_2C_5H_3$ ligand is localized at two positions which allows more effective room for polymerization activity. On the other hand, it should be noted that $(C_5Me_5)_2Sm$, which has even more room for polymerization, does not form solid polymer at a faster rate. Hence, Sm^{II}-based alkene polymerizations may be very sensitive to the local environment around the metal.

The reactivity of $[(Me_3Si)_2C_5H_3]_2Sm(THF)$ with CO is not parallel to that of the pentamethylcyclopentadienyl Sm^{II} complexes, however. Instead of forming a complex of an anion derived from reductive homologation of CO as in eq. 1, **1** forms the tris(cyclopentadienyl) complex **3**. In this sense, $[(Me_3Si)_2C_5H_3]_2Sm(THF)$ is like $[(Me_3Si)_2N]_2Sm(THF)_2$ [11] and $SmI_2(THF)_2$ [10], both of which form tris ligand Sm^{III} species as reaction products with CO [11,12]. Indeed, one of the key features of the reactivity of the $(C_5Me_5)_2Sm(THF)_x$ complexes may be the fact that $(C_5Me_5)_3Sm$ species do not form as reaction products. It has been calculated that $(C_5Me_5)_3Sm$ is too sterically crowded to exist [42]. This idea is supported by the X-ray crystal structure of $(C_5Me_5)_2Sm(C_5H_5)$ (**5**) [49]. In **5**, the 127.0° (C_5Me_5 ring centroid)–Sm–(C_5Me_5 ring centroid) angle is one of the smallest observed for trivalent $(C_5Me_5)_2Sm$ complexes, a fact which suggests significant steric crowding. Replacement of the C_5H_5 ligand by C_5Me_5 would increase the crowding further.

Prior to this study, it was not known if the bis(trimethylsilyl)cyclopentadienyl ligand would form a tris ligand complex with a metal as small as Sm^{3+}. Results in U^{III} chemistry led to the suggestion that the $C_5H_3(SiMe_3)_2$ ligand was more sterically demanding than C_5Me_5 [20]. On the other hand, as discussed above, the steric bulk in $C_5H_3(SiMe_3)_2$ is more localized than in C_5Me_5. The isolation of the actinide complex $[(Me_3Si)_2C_5H_3]_3An$ (An = Th [19], U [50]) showed that this ligand could form tris cyclopentadienyl complexes. As shown in Fig. 2, the steric bulk in **3** can be spread out such that a triscyclopentadienyl complex can form even with a metal the size of Sm^{III}.

Conclusion

Although the sterically bulky bis(trimethylsilyl)cyclopentadienyl ligand provides a soluble Sm^{II} complex analogous to $(C_5Me_5)_2Sm(THF)$, the reactivity of $[(Me_3Si)_2C_5H_3]_2Sm(THF)$ is not always similar. With some substrates, the localized steric bulk in the $(Me_3Si)_2C_5H_3$ ligand may allow higher rates of reactivity. In other reactions, the availability of the tris(cyclopentadienyl) complex (**3**) provides an alternative reaction pathway for $[(Me_3Si)_2C_5H_3]_2Sm(THF)$ which is not apparently available to $(C_5Me_5)_2Sm(THF)$. In such reactions, the special chemistry possible with the $(C_5Me_5)_2Sm(THF)_x$ complexes may be associated with the inaccessibility of $(C_5Me_5)_3Sm$. The two types of substituted cyclopentadienyl ligands appear to provide complementary opportunities for exploiting the reactivity of Sm^{II}.

Acknowledgment

We thank the National Science Foundation for support of this research. Funds for the purchase of the Nicolet R3m/V diffractometer system were made available from the National Science Foundation under Grant CHE-85-14495.

References

1 W.J. Evans, I. Bloom, W.E. Hunter and J.L. Atwood, J. Am. Chem. Soc., 103 (1981) 6507.
2 W.J. Evans, J.W. Grate, H.W. Choi, I. Bloom, W.E. Hunter and J.L. Atwood, J. Am. Chem. Soc., 107 (1985) 941.
3 W.J. Evans, L.A. Hughes and T.P. Hanusa, J. Am. Chem. Soc., 106 (1984) 4270.
4 W.J. Evans, L.A. Hughes and T.P. Hanusa, Organometallics, 5 (1986) 1285.
5 W.J. Evans, in K.S. Suslick (Ed.), High-Energy Processes in Organometallic Chemistry, ACS Symp. Ser., 333 (1987) 278.
6 W.J. Evans, J.W. Grate, L.A. Hughes, H. Zhang and J.L. Atwood, J. Am. Chem. Soc., 107 (1985) 3728.
7 W.J. Evans, L.A. Hughes, D.K. Drummond, H. Zhang and J.L. Atwood, J. Am. Chem. Soc., 108 (1986) 1722.
8 W.J. Evans, D.K. Drummond, L.R. Chamberlain, R.J. Doedens, S.G. Bott, H. Zhang and J.L. Atwood, J. Am. Chem. Soc., 110 (1988) 4983.
9 A. Recknagel, D. Stalke, H.W. Roesky and F.T. Edelman, Angew. Chem., Int. Ed. Engl., 28 (1989) 445.
10 J.L. Namy, P. Girard, H.B. Kagan and P.E. Caro, Nouv. J. Chimie, 5 (1981) 479.
11 W.J. Evans, D.K. Drummond, H. Zhang and J.L. Atwood, Inorg. Chem., 27 (1988) 575.
12 W.J. Evans and T.A. Ulibarri, unpublished results.
13 E.W. Abel and M.O. Dunster, J. Organomet. Chem., 33 (1971) 161.
14 Y.A. Ustynyuk, A.V. Kisin, I.M. Pribytkova, A.A. Zekin and N.D. Antonova, J. Organomet. Chem., 42 (1972) 47.
15 M.F. Lappert, A. Singh, J.L. Atwood and W.E. Hunter, J. Chem. Soc., Chem. Commun., (1981) 1190.
16 M.F. Lappert, A. Singh, J.L. Atwood and W.E. Hunter, J. Chem. Soc., Chem. Commun., (1981) 1191.
17 M.F. Lappert, A. Singh, J.L. Atwood, W.E. Hunter and H.-M. Zhang, J. Chem. Soc., Chem. Commun., (1983) 69.
18 M.F. Lappert, A. Singh, J.L. Atwood and W.E. Hunter, J. Chem. Soc., Chem. Commun., (1983) 206.
19 P.C. Blake, M.F. Lappert, J.L. Atwood and H. Zhang, J. Chem. Soc., Chem. Commun., (1986) 1148.
20 P.C. Blake, M.F. Lappert, R.G. Taylor, J.L. Atwood, W.E. Hunter and H. Zhang, J. Chem. Soc., Chem. Commun., (1986) 1394.
21 W.K. Kot, G.V. Shalimoff, N.M. Edelstein, M.A. Edelman and M.F. Lappert, J. Am. Chem. Soc., 110 (1988) 986.
22 P.C. Blake, E. Hey, M.F. Lappert, J.L. Atwood and H. Zhang, J. Organomet. Chem., 353 (1988) 307.
23 W.J. Evans, L.R. Chamberlain, T.A. Ulibarri and J.W. Ziller, J. Am. Chem. Soc., 110 (1988) 6423.
24 T.L. Brown, D.W. Dickerhoof, D.A. Bafus and G.L. Morgan, Rev. Sci. Inst., 33 (1962) 491.
25 M.D. Taylor and C.P. Carter, J. Inorg. Nucl. Chem., 24 (1962) 387.
26 W.J. Evans and T.A. Ulibarri, Polyhedron, 8 (1989) 1007.
27 W.J. Evans, J.W. Grate and R.J. Doedens, J. Am. Chem. Soc., 107 (1985) 1671.
28 M.R. Churchill, R.A. Lashewycz and F.J. Rotella, Inorg. Chem., 16 (1977) 265.
29 UCLA Crystallographic Computing Package, University of California, Los Angeles, 1981, C. Strouse, personal communication.

30 Nicolet Instrument Corporation, Madison, Wisconsin, 1987.

31 International Tables for X-ray Crystallography, Kynoch Press, Birmingham, England, 1974; (a) pp. 99–101; (b) pp. 149–150.

32 P.W.R. Corfield, R.J. Doedens and J.A. Ibers, Inorg. Chem., 6 (1967) 197.

33 M.R. Churchill, Inorg. Chem., 12 (1973) 1213.

34 P.L. Watson and T. Herskovitz, ACS Symp. Ser., 212 (1983) 459.

35 W.J. Evans, T.A. Ulibarri and J.W. Ziller, J. Am. Chem. Soc., 112 (1990) 2314.

36 W.J. Evans, Polyhedron, 6 (1987) 803.

37 R.D. Shannon, Acta Crystallogr., Sect. A, 32 (1976) 751.

38 T.J. Marks and R.D. Ernst, in G. Wilkinson, F.G.A. Stone and E.W. Abel (Eds.), Comprehensive Organometallic Chemistry, Pergamon Press, Oxford, 1982, Ch. 21.

39 W.J. Evans, Adv. Organomet. Chem., 24 (1985) 131.

40 H. Schumann and W. Genthe, in K.A. Gschneidner, Jr. and L. Eyring (Eds.), Handbook on the Physics and Chemistry of Rare Earths, Elsevier, Amsterdam, 1985, Vol. 7, Ch. 53 and references therein.

41 A.L. Wayda and W.J. Evans, Inorg. Chem., 19 (1980) 2190.

42 T.D. Tilley and R.A. Andersen, Inorg. Chem., 20 (1981) 3267.

43 G. Jeske, H. Lauke, H. Mauermann, P.N. Swepston, H. Schumann and T.J. Marks, J. Am. Chem. Soc., 107 (1985) 8091.

44 H.J. Heeres, A. Meetsma and J.H. Teuben, J. Chem. Soc., Chem. Commun., (1988) 962.

45 M.D. Rausch, K.J. Moriarity, J.L. Atwood, J.A. Weeks, W.E. Hunter and H.G. Brittain, Organometallics, 5 (1986) 1281.

46 P.N. Hazin, J.C. Huffman and J.W. Bruno, Organometallics, 6 (1987) 23.

47 W.J. Evans, J.M. Olofson, H. Zhang and J.L. Atwood, Organometallics, 7 (1988) 629.

48 G.W. Watt and E.W. Gillow, J. Am. Chem. Soc., 91 (1969) 775.

49 W.J. Evans and T.A. Ulibarri, J. Am. Chem. Soc., 109 (1987) 4292.

50 S.M. Beshouri, R.A. Andersen, N.M. Edelstein, W. Kot, P. Matsunaga and A. Zalkin, 196th Meeting of the American Chemical Society, Los Angeles, California, September 1988, INOR 177.